PROJECT REPORT

Experiment Ref. No. CH 3386
Title: “pH-driven transitions in biopolymer-based 'smart' nanoparticles at the mesoscopic scale”

Beamline: BM02

Dates: 21 – 23 October 2011

Research Team

Dr. Francisco M. Goycoolea (WWU, Germany)
Dr. Cyrille Rochas (CNRS, France)
Dr. David Laurent (U.Lyon, France)
Juan Pablo Fuenzalida (WWU, Germany)
Bianca Menchicchi (WWU, Germany)
Celina Vila (WWU, Germany)
Giovanni Zorzi (WWU, Germany)
Daniella Morgado (U.Lyon, France)
Edison Kato (U.Lyon, France)

Abstract

As a part of a project focused on the design of novel biopolymer-based nanoparticle systems with bioresponsive properties for advanced drug delivery application, synchrotron SAXS studies have allowed to deepen our understanding of the structure of various nanoparticles comprising chitosan, alginate and proteins such as insulin, lysozyme and glycoproteins such as mucin at varying pH and ionic strength.

Introduction

In previous synchrotron SAXS studies conducted in 2009 (Proposal No. SC-2774) at beamline BM02 unpredictable results were obtained for gelled nanoparticle systems comprising different polysaccharide and when these were subjected to varying pH. The existence of a core-shell morphology in the various nanoparticle systems was inferred from the goodness of fit of the corresponding model used to describe the intensity scattering curves in a given q region, particularly in systems that comprised either chitosan or in those comprising chitosan and alginate and in both cases when a chemical crosslinking agent, genipin, was used to modify the surface of the harnessed particles. The thickness of the formed shell was found to be influenced by the composition of the system, the pH and the ionic strength.
In these new experiments, we have refined and expanded the former studies, with particular attention to the following aspects:

a) By deepening our understanding of the surface molecular topolgy, interactions and structure of the nanoparticles modelled as centrosymmetric spheres of with radial variation of electron density.[1]
b) By characterizing the sensitivity of the nanoparticles towards changes in composition of the polyelectrolytes, crosslinking agents and presence of protein/peptide macromolecules, particularly, insulin, lysozyme and a glycoprotein, mucin.
c) By characterizing pH- and salt-induced transitions in terms of the dimensions of their core and shell in a range of pH emulating physiological conditions.
d) By initiating preliminary studies focused on modified proteins with affinity to chitosan.

Experimental

Instrument settings at BM02

Beamline: BM02

Instrument settings
E = 16 kEv (λ =0.785 Å)
Sample-to-detector distance: 188 cm
Beam stop = 3
LN = 100 kHz

The collected scattering data were calibrated on the basis of the known positions of silver behenate powder Bragg reflections (*d*=58.376 Å).

The following experiments were conducted:

Experiment I. Nanoparticles comprising chitosan (CS), alginate (Mw 18000 Da) formed by ionotropic gelation with pentasodium triplyphosphate (TPP) and also with genipin. These particles were loaded with bovine insulin. The particles were studied under physiological conditions at varying pH in the appropriate buffer systems, namely:

a) Simulated gastric fluid pH 1.2 (without enzymes)
b) Simulated intestinal fluid pH 6.8 (without enzymes)

Experiment II. Studies on nanocomplex systems of alginate – mucin at varying mucin/alginate mass ratios.

Experiment III. Studies on nanocomplex systems of alginate – lysozyme at lysozyme/alginate equivalent charge ratio of 0.285 and a total amount of charge in solution of 6 meq/L.

Experiment IV. Chitin affinity protein – green fluorescent protein (CAP-eGFP) in the absence and in the presence of chitosan oligomer substrate in TRIS buffered saline (TBS) pH 7.5.

Results and discussion

Experiment I

The SAXS intensity curves of CS-TPP-alginate nanoparticles either blank or loaded with insulin and either surface crosslinked or not were recorded in simulated gastric fluid (pH 1.2) or in simulated intestinal fluid (pH 6.8). But as the slope of the plot *log I* vs *log q* invariable assumend values larger than 4.0, the classical Porod's treatment is not applicable and a modified core-shell model had to be used whereby the interfacial thickness of the NPs could be calculated, using the following equation[2,3]:

$$I(q) * q^2 = -B + \frac{1}{q^2} * C \qquad (1)$$

Where C and B are the Porod's and the interface constants, respectively.

The value of the interface of transition layer (shell) L_i can be calculated from the expression:

$$L_i = \sqrt{B \frac{12\pi}{C}} \qquad (2)$$

The result of this analysis is shown in Figure 1. For all the nanoparticles studied in this experiment, it was was possible to fit the core-shell model and estimate average values of shell thickness. Figure 2 shows the summary of these analysis for the various addressed nanoparticles. Transmission electron microscopy (TEM) studies (Figure 3) does not allow core shell structure does exist in CS-TPP based nanoparticles. The insulin release behavior of these nanoparticle systems has also been addressed and has revealed that the systems that are crosslinked with genipin are able to retain insulin in SGF, while those which are not crosslinked, release the protein almost immediately under these conditions. This behavior cannot be ascribed to a change in the nanoparticle shell thickness, as no differences were noticed between uncrosslinked and crosslinked nanoparticles (Figure 2). It was interesting to notice, however, that in simulated intestinal fluid (pH 6.8), the insulin loaded nanoparticles that were crosslinked exhibited a larger interfacial thickness than

that attained in SGF and also than the non-crosslinked particles in SIF. These differences reveal that the shell of the particles is able to react to the external environment and that changes in the degree of protonation of chitosan, alginate and insulin are surely at play in determining the behavior of these systems. Ultimately, a better understanding of the underlying mechanisms at molecular level, shall lead to the better tuning of the stability and drug release properties of these systems.

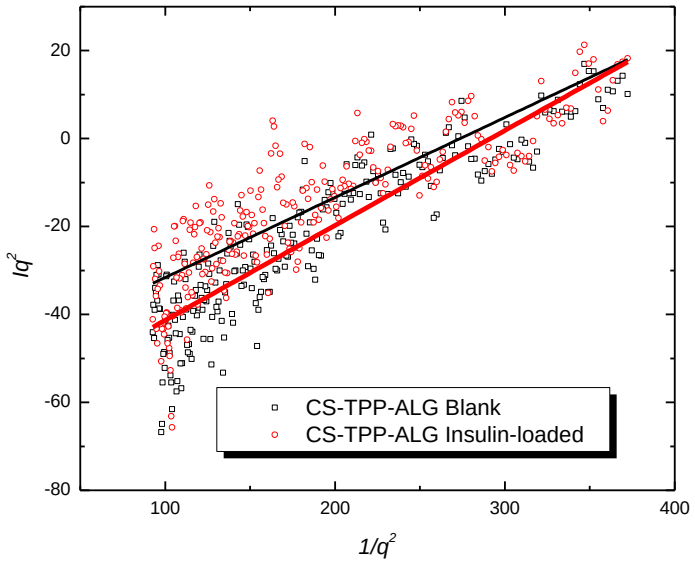

Figure 1. Core-shell model plots ($I(Q)Q^2$ vs. $1/Q^2$) applied to SAXS scattering curves for CS-TPP-ALG blank and insulin-loaded nanoparticles.

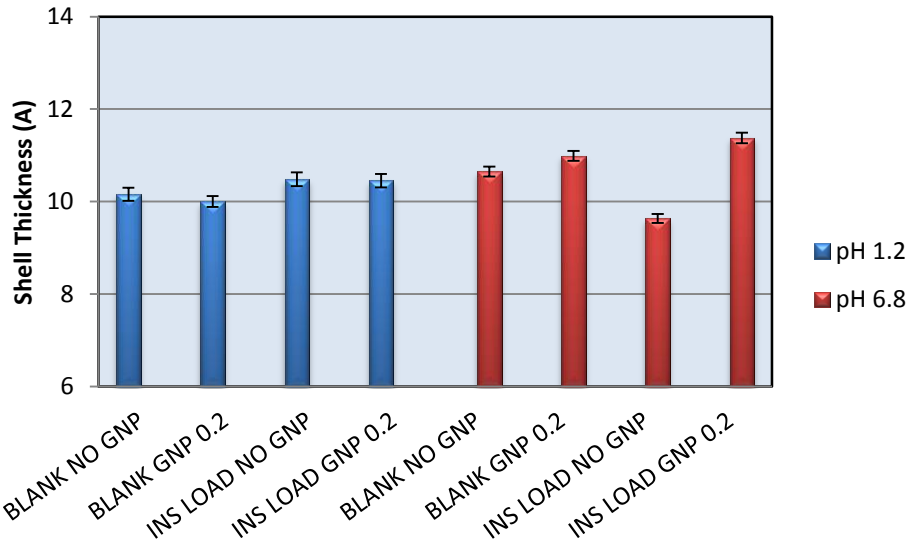

Figure 2. Average shell thickness for CS-TPP-ALG blank and insulin-loaded nanoparticles in simulated gastric fluid (pH 1.2) and in simulated intestinal fluid (pH 6.8).

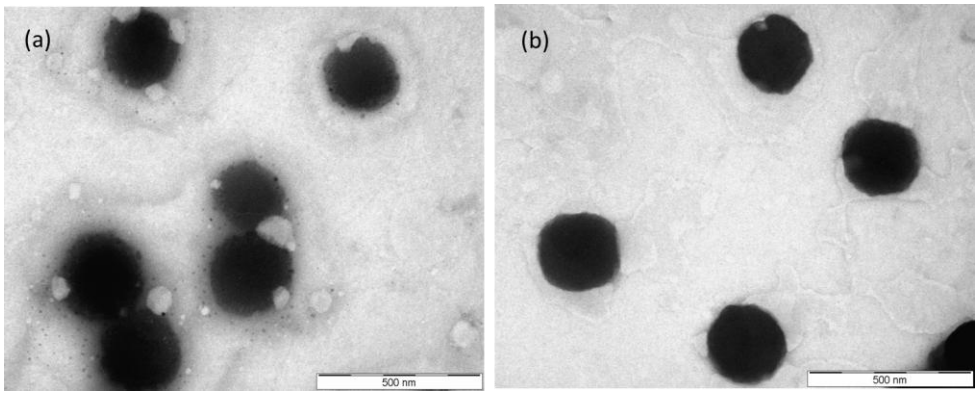

Figure 3. Transmission electro microscopy (TEM) images of a: CS-TPP-polyelectrolyte insulin loaded nanoparticles without genipin crosslinking and b) CS-TPP-polyelectrolyte insulin loaded nanoparticles crosslinked with genipin.

Experiment III.

The molecular interactions between the soluble fraction of porcine gastric mucin when mixed at varying mass ratio with different polysaccharides are being currently investigating by rheological methods. An interaction between mucin and alginate has been hypothesized to occur, particularly at mucin/alginate mass ratios > ca. 0.7. Differences in the interaction behavior have also been observed as a function of the Mw of alginate, pH and ionic strength.
For a better understanding of these phenomena, SAXS experiments were carry out. The scattering intensity obtained can be represented by the Ornstein–Zernike (OZ) equation (Eq. 3) describing the scattering behavior of a gel in dilute conditions or semi diluted solutions.[4,5]

$$I(q) = \frac{I_0}{1 + \zeta^2 q^2} \qquad (3)$$

Where, *I*(*q*) is the observed corrected intensity at a given *q* value, *Io* is the incident initial intensity, ζ is the mesh size. Table 1 summarizes the results of these experiments.

Table 1. Mesh size of mucin and mucin-alginate systems as determined by SAXS

System	***Mesh(nm)***	***Relative Viscosity mPa/s***
Mucin	5.38	2.130
Mucin-Alginate (f=0,9)	7.15	1.702
Mucin-Alginate (f=0,8)	7.67	1.776

f represents the mucin/alginate mass ratio

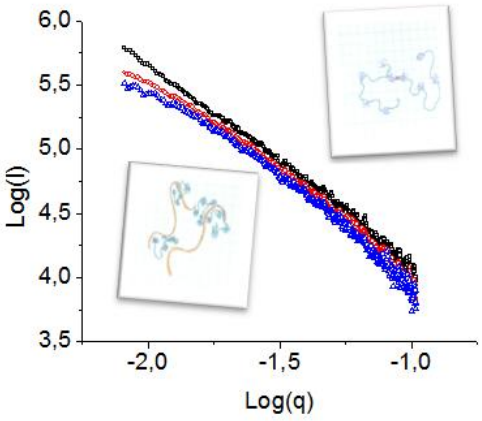

Figure 4. SAXS intensity scattering curves for: black line: mucin solution, red line: mucin-alginate f= 0.9 and blue line: mucin-alginate f= 0.8

Figure 4 shows a linearization of the OZ equation for mucin and for alginate-mucin systems wehereby one can calculate the mesh size of the blob, meaning the space in which a single polymeric chain does not interact with other chains. In the Figure 4 represented the scattering pattern of the solutions of mucin alone and in the presence of 10% alginate (Mw 102 kDa). Reorganization of the chains and conformational changes of tertiary structure of mucin seem to be at play to modify the mesh size values and this can be due to the presence of the interacting polymer or simply due to a dilution effect. In a new experiment it would be important to test several concentration of samples and different ratio for clarify if this effect due to a dilution effect or a change in the distribution of the polymer in solutions and also try to found a correlation model between the data obtain by SAXS and the once obtained by viscosimetry.[6]

Experiment IV

Nanocomplexes (NCXs) made of alginate (Mw 4 kDa) – lysozyme at a charge ratio of 0.285 and a total amount of charge in solution of 6 meq/L with an average size of 225 ±3.7 nm and surface zeta potential of -35 ± 3 mV were addressed. NCXs were diluted with NaCl solution to afford a 4mM concentration of NaCl. Both NCXs systems exhibited a negative zeta potential, diagnostic evidence to the preferential occurrence of alginate on the surface. The SAXS experiment allowed us to observe only the Porod's law region (where Eq. 4 is met) and not the Guinier's one, due to the large size of the NPs using the following equation:[7]

$$I(q) = \frac{I_0}{q^4} \qquad (4)$$

But as the slope is larger than 4.0 (Figure 5C), the classical Porod's treatment is not applicable. The interpretation of this value is concordant whit interfacial transition between the NPs and the solvent. The use of the modified Porod's law (Eq. 1) allowed us to obtain the interfacial thickness of the NPs, using the plot shown in Figure 5 B and applying equation 1 used to treat the CS-TPP-alginate nanoparticle systems of experiment I above.

The decrease in the size of the shell observed in Figure 5 B can be correlated to the reorganization of alginate chain in the surface of the particle due to the increase in the ionic strength and also to the binding between of sodium ions with the guluronic unit present in alginate. To investigate in greater depth this NCX system, a new comparative SAXS study with alginates of different Mw and mannuronic and guloronic acid (M/G) ratios will be extremely informative.

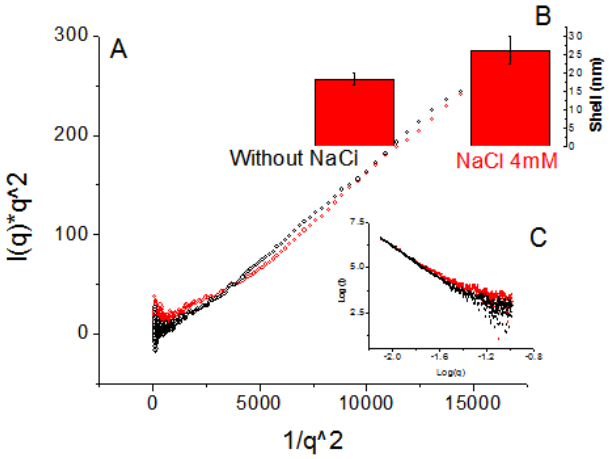

Figure 5. Nanocomplex system lysozyme-alginate at charge ratio 0.285 and total amount of charge of 6 meq/L , A: modified Porod's plot, B: shell thicknes in systems without and with 4 mM NaCl, C: Plot of the same data as in A in the form Log I(q) vs Log q

Experiment V.

Preliminary experiments were initiated in the characterization of a new type of proteins that are being engineered in our Institutue at WWU with a view to use them as fluorescent labeling tools for chitin- and chitosan-based nanosystems. It was possible conduct SAXS measurements in the protein in both situations, in the free state and when bound to its substrate.

Figure 6 shows the SAXS intensity scattering curves for the CAP-GFP and CAP-GFP bound to chitosan oligomer. Clearly, in both systems it is possible to observe the Guinier region at low q values. The insert shows the linearized form

of Guniers plot (log I vs q^2), from which it is possible to obtain the radius of gyration of the systems, according with the following equations[7]

$$I = Ie^{q^2} * \frac{-Rq^2}{3} \quad (5)$$

$$Log(I) = Log(I_0) - q^2 \frac{Rg^2}{3 * Ln(10)} \quad (6)$$

The obtained results are shown in Table 2.

Table 2. Radius of gyration (Rg) of CAP-GFP and CAP-GFP bound to chitosan oligomer

	Radius of gyration(nm)	S.E.
CAPGFP CS	5.906	0.273
CAPGFP	6.531	0

It is interesting to notice that when the CAP-GFP protein is bound to its substrate, a reduction in R_g equivalent to 0.625 nm is observed. To a first approximation, the differences in dimensions between the bound and free state of the protein may reflect structural changes which may be possibly associated to a slight change in conformation as the chitosan oligomer binds to CAP binding site. Differences in the order of 0.4 nm (4 Å) have been documented for varying conformational states of phosphoglycerate kinase (PGK), the enzyme responsible for the first ATP-generating step of glycolysis, upon complexing to its substrate.[8] These preliminary results allow to anticipate that it would be extremely interesting to proble by SAXS the interactions between chitosan longer polymer chains and chitosan-based nanoparticles in solution.

SUBMITTED PUBLICATIONS

Goycoolea F.M., Valle-Gallego A., Stefani R., Mencicchi B., David L., Rochas C., Santander-Ortega M.J., Alonso M.J. Chitosan–based nanocapsules: Physical characterization, stability in biological media and capsaicin encapsulation. Submitted to *Colloid and Polymer Science*.

Reference List

1. Clark A. In: *Physical techniques for the study of food biopolymers*. Ross-Murphy S. B. (Ed.). Blackie Academic Professional. London. 65-149
2. Kim, M.H. Modified Porod's law estimate of the transition-layer thickness between two phases: test of triangular smoothing function *Journal of Applied Crystallography* (2004) 37, 643-651.
3. Alexandre Drogoz, Séverine Munier, Bernard Verrier, Laurent David, Alain Domard, and Thierry Delair. Towards Biocompatible Vaccine Delivery Systems: Interactions of Colloidal PECs Based on Polysaccharides with HIV-1 p24 Antigen. *Biomacromolecules* 2008 9 (2), 583-591
4. Gennes, P. G. d. *Scaling Concepts in Polymer Physics* (1979) p 324
5. Schuster E., Cucheval A., Lundin L., Williams M.A.K. Using SAXS to Reveal the Degree of Bundling in the Polysaccharide Junction Zones of Microrheologically Distinct Pectin Gels, *Biomacromolecules* 2011 12 (7), 2583-2590
6. Draget K.I., Stokke B.T., Yuguchi Y., Urakawa H. Kajiwara K. Small-Angle X-ray Scattering and Rheological Characterization of Alginate Gels. 3. Alginic Acid Gels, *Biomacromolecules* 2003 *4* (6), 1661-1668
7. O. Glatter and O. Kratky *Small angle X ray scattering.* Academic Press Inc. (1982).
8. Zerrad L., Merli A., Schroöder G.F., Varga A., Gráczer E., Pernot P., Round A., Vas M. and Bowler M.W. A Spring-loaded Release Mechanism Regulates domain Movement and Catalysis in Phosphoglycerate Kinase. *J. Biol. Chem.* 286, 14040–14048.